

# Cluster model and band structure calculations of $V_2O_5$ : Reduced $V^{5+}$ symmetry and many-body effects

R. J. O. Mossaneck,<sup>1</sup> A. Mocellin,<sup>2</sup> M. Abbate,<sup>1,\*</sup> B. G. Searle,<sup>3</sup> P. T. Fonseca,<sup>4</sup> and E. Morikawa<sup>5</sup>

<sup>1</sup>*Departamento de Física, Universidade Federal do Paraná, Caixa Postal 19081, 81531-990 Curitiba, Parana, Brazil*

<sup>2</sup>*Instituto de Física, Universidade de Brasília, Caixa Postal 04455, 70919-970 Brasília, Distrito Federal, Brazil*

<sup>3</sup>*Computational Science and Engineering Department, STFC Daresbury Laboratory, Warrington WA4 4AD, United Kingdom*

<sup>4</sup>*Laboratório Nacional de Luz Síncrotron, Caixa Postal 6192, 13084-971 Campinas, São Paulo, Brazil*

<sup>5</sup>*Center for Advanced Microstructures and Devices, Louisiana State University, Baton Rouge, Louisiana 70806, USA*

(Received 7 August 2007; revised manuscript received 2 October 2007; published 15 February 2008)

We studied the electronic structure of the  $V_2O_5$  compound using cluster model calculations. The calculation included the reduced  $V^{5+}$  symmetry and the strong  $V 3d-O 2p$  covalence effects. The many-body effects are taken into account using the configuration interaction method. The ground state of  $V_2O_5$  is highly covalent and dominated by the  $3d^1\bar{L}$  ( $^1A_1$ ) configuration, where  $\bar{L}$  denotes a ligand hole. The  $V_2O_5$  material is in the charge-transfer regime and the band gap is due to  $p-d$  transitions. The first removal state is given by the  $3d^0\bar{L}$  ( $^2A_1$ ) configuration, and the first addition state is formed by the  $3d^1$  ( $^2E$ ) configuration. The results of the cluster model are in good agreement with band structure calculations. The calculation results are also in good agreement with photoemission and x-ray absorption spectra. The  $V 2p$  core-level spectra exhibit many-body effects despite the nominal  $3d^0$  occupancy. These effects and the reduced  $V^{5+}$  symmetry are crucial to describe the electronic structure of  $V_2O_5$ .

DOI: [10.1103/PhysRevB.77.075118](https://doi.org/10.1103/PhysRevB.77.075118)

PACS number(s): 71.28.+d, 71.70.Ch, 79.60.Bm, 78.70.Dm

## I. INTRODUCTION

The vanadium oxide family forms many different compounds with a broad range of physical properties. The interest in this kind of materials is often related to the presence of a metal-insulator transition (MIT).<sup>1</sup> Although it does not present a MIT transition, the  $V_2O_5$  compound is one of the most widely studied. The studies on this material are mostly focused in its applications in Li-ion batteries,<sup>2</sup> electrochromic devices,<sup>3</sup> gas sensors,<sup>4</sup> and supported catalysis.<sup>5</sup>

The structure of the  $V_2O_5$  material is orthorhombic with the  $V^{5+}$  ions in a square pyramid coordination.<sup>6</sup> The structure consists of layers formed by these square pyramids and presents a strong two-dimensional character. The  $V_2O_5$  compound is a semiconductor with a band gap of approximately 2.2–2.3 eV.<sup>7,8</sup> The electronic structure of  $V_2O_5$  was studied experimentally using photoemission,<sup>9,10</sup> resonant photoemission,<sup>11</sup> x-ray absorption,<sup>12,13</sup> photoemission and Auger,<sup>14</sup> x-ray emission,<sup>15</sup> x-ray appearance near edge structure and extended x-ray absorption fine structure,<sup>16,17</sup> and electron-energy-loss<sup>18</sup> spectroscopy.

The electronic structure of  $V_2O_5$  was studied theoretically using band structure<sup>19,20</sup> and cluster model<sup>21,22</sup> calculations. These calculations showed the crucial relationship between the crystal structure and the electronic structure. The  $V 2p$  x-ray photoelectron spectrum of  $V_2O_5$  was analyzed using cluster model calculations.<sup>23</sup> This calculation method included explicitly many-body effects and the strong  $V 3d-O 2p$  hybridization, but it did not include the correct local  $V^{5+}$  symmetry and it was restricted to the  $V 2p$  core-level spectrum.

The aim of this work is to study the electronic structure of  $V_2O_5$  using cluster model calculations. The approach includes now the reduced symmetry of the  $V^{5+}$  ions and also relevant many-body effects. These two effects are com-

pletely necessary to describe the electronic structure of the  $V_2O_5$  compound. The cluster model results are in good agreement with band structure calculations, as well as with the experimental photoemission and x-ray absorption spectra. The calculated band gap mainly has a  $p-d$  character and is in good agreement with the experimental value.

## II. EXPERIMENTAL DETAILS

The samples were  $V_2O_5$  polycrystals with large and highly oriented needlelike grains. These polycrystals were obtained from the melt in air at 650 °C and cooled down at 1 °C/min. The subsequent powder x-ray diffraction analysis showed that the resulting samples were single phase.

The photoemission spectrum was measured at the plane-grating monochromator beamline in CAMD. The photon energy was set to 50 eV, the energy resolution was about 0.4 eV, and the energy scale was calibrated using the Fermi level of a gold foil. The x-ray photoelectron spectrum was measured using Mg  $K\alpha$  radiation in a conventional equipment. The energy resolution was about 0.9 eV, and the energy scale was calibrated using the peak positions of a Ag foil.

The x-ray absorption spectra were measured at the spherical-grating monochromator beamline in LNLS. The energy resolution was about 0.5 eV, and the energy scale was calibrated using the known  $V_2O_5$  peak positions. The sample was scrapped with a diamond file in all cases to remove the surface contamination. All the spectra presented here were normalized to the maximum after a constant background subtraction.

## III. CALCULATION DETAILS

### A. $V^{5+}$ ion symmetry

The transition metal ions in oxides usually appear in  $MO_6$  blocks with an octahedral local symmetry. The resulting  $O_h$

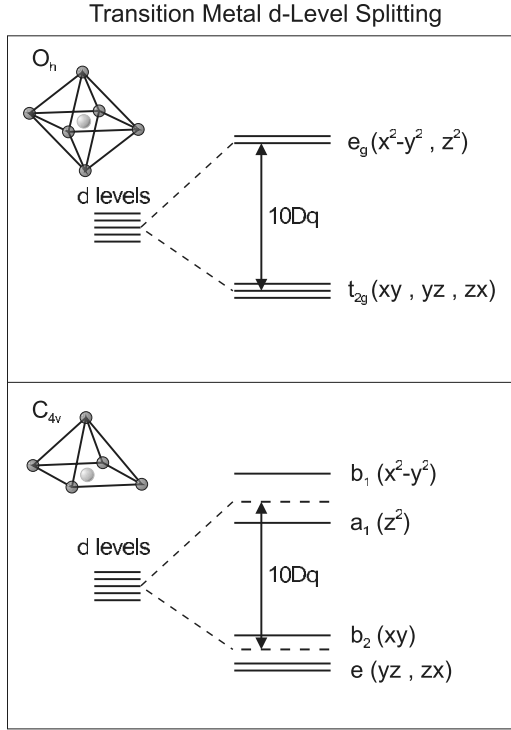


FIG. 1. Splitting of the transition metal  $d$  levels in  $O_h$  and  $C_{4v}$  symmetries.

crystal field, given by the  $Dq$  parameter, splits the  $M d$  orbitals into the  $t_{2g}$  and  $e_g$  levels (see Fig. 1). Many transition metal oxides present distortions within the  $MO_6$  octahedra and/or alterations in the way these  $MO_6$  blocks are connected together. These lattice distortions are responsible for changes in the physical properties of these compounds.

The  $VO_6$  block in the  $V_2O_5$  compound presents a rather large deviation from octahedral symmetry. In fact, one of the apical oxygen ions is so far away that the corresponding V-O interaction is much weaker. Thus, it is more appropriate to use a  $VO_5$  square base pyramid as a block to describe the  $V_2O_5$  compound. The resulting  $C_{4v}$  crystal field, given by the  $Dq$ ,  $Ds$ , and  $Dt$  parameters, produces an additional splitting (see Fig. 1). The relative energy position of the different V  $3d$  levels in  $C_{4v}$  symmetry is given in Table I.

### B. Cluster model

The cluster consisted of a  $[VO_5]^{-5}$  square base pyramid structure resulting in a  $V^{5+}$  ion with a nominal  $3d^0$  occupancy. The model was solved using the configuration inter-

TABLE I. Energy position of the different V  $3d$  levels in  $C_{4v}$  symmetry.

| Level           | Position          |
|-----------------|-------------------|
| $b_1 (x^2-y^2)$ | $6 Dq+2 Ds-1 Dt$  |
| $a_1 (z^2)$     | $6 Dq-2 Ds-6 Dt$  |
| $b_2 (xy)$      | $-4 Dq+2 Ds-1 Dt$ |
| $e (yz,zx)$     | $-4 Dq-1 Ds+4 Dt$ |

TABLE II. Model parameters used in the calculations of  $V_2O_5$ .

| Parameter            | Value (eV) |
|----------------------|------------|
| $\Delta$             | 0.70       |
| $U$                  | 5.5        |
| $pd\sigma$           | 2.7        |
| $Dq$                 | 0.15       |
| $Ds$                 | 0.10       |
| $Dt$                 | 0.04       |
| $pp\pi$ - $pp\sigma$ | 0.70       |

action method, which includes relevant many-body effects.<sup>24,25</sup> The ground state  $\Phi_i$  was expanded in the following configurations:  $3d^0$ ,  $3d^1L$ ,  $3d^2L^2$ ,  $3d^3L^3$ , etc., where  $L$  denotes a hole in the O  $2p$  band. The main parameters of the model were the charge-transfer energy  $\Delta$ , the Mott-Hubbard repulsion  $U$ , the  $p$ - $d$  transfer integral ( $pd\sigma$ ), and the core-hole potential  $Q$  ( $Q=1.25U$ ).<sup>23</sup> The multiplet splitting was obtained in terms of the crystal field parameters  $Dq$ ,  $Ds$ , and  $Dt$ , as well as the  $p$ - $p$  transfer integral ( $pp\pi$ )-( $pp\sigma$ ).

The final states ( $\Phi_f$ ) were obtained by removing a V  $3d$  electron (photoemission spectroscopy), adding a V  $3d$  electron (BIS), adding an O  $2p$  electron [O  $1s$  x-ray absorption spectroscopy (XAS)], removing a V  $2p$  electron (V  $2p$  x-ray photoemission spectroscopy), and removing (adding) a V  $2p$  ( $3d$ ) electron (V  $2p$  XAS). The corresponding spectral weight  $A(\omega)$  for each case was calculated using the sudden approximation,

$$I(\varepsilon) = \sum_f |\langle \Phi_f | \hat{O} | \Phi_i \rangle|^2 \delta(\varepsilon - E_f + E_i), \quad (1)$$

where  $\Phi_i (E_i)$  is the ground state vector (energy),  $\Phi_f (E_f)$  is the  $f$ th final state vector (energy), and  $\hat{O}$  is the corresponding transition operator. The same approach was recently used to describe the electronic structure of  $VO_2$  and  $V_2O_3$ .<sup>26,27</sup>

The values of the model parameters used in the calculation of  $V_2O_5$  are listed in Table II (it is worth noting that the same set of parameters was used in all the calculations presented here). These values gave the best agreement with the experiment and are similar to previous estimates.<sup>23</sup> Further, these parameters follow the expected chemical trend in the  $V_2O_5$ - $VO_2$ - $V_2O_3$  series.<sup>23</sup>

### C. Band structure

The band structure was calculated using the standard local density approximation (LDA). The program used the full-potential linear-muffin-tin orbital method.<sup>28</sup> The exchange and correlation potential was calculated using the Vosko approximation.<sup>29</sup> The calculation was performed in the observed orthorhombic structure (space group  $Pmmn$ ). The lattice parameters and atomic positions used in the calculation are given in Table III. The basis set for the valence electrons

TABLE III. Lattice parameters and atomic positions used in the band structure calculation of  $V_2O_5$ .

| Parameter           | Value (Å)            |
|---------------------|----------------------|
| $a$                 | 11.512               |
| $b$                 | 3.564                |
| $c$                 | 4.368                |
| Atom                | Position             |
| V (4f)              | 0.101, 0.250, -0.108 |
| O <sub>v</sub> (4f) | 0.104, 0.250, -0.469 |
| O <sub>c</sub> (4f) | -0.069, 0.250, 0.003 |
| O <sub>b</sub> (2a) | 0.250, 0.250, 0.001  |

were  $4s$ ,  $4p$ , and  $3d$  for V and  $2s$ ,  $2p$ , and  $3d$  for O. The self-consistent potential and the density of states were calculated using 64 irreducible  $\mathbf{k}$  points.

#### IV. RESULTS AND DISCUSSION

The calculated contribution of the main configurations to the ground state of  $V_2O_5$  is given in Table IV. The ground state of  $V_2O_5$  is dominated by the  $3d^1L$  and  $3d^2L^2$  configurations with a contribution of 75%. The relatively large weight of these configurations indicates that  $V_2O_5$  is in the charge-transfer regime.<sup>30</sup> This conclusion is also supported by the relative value of the  $\Delta$  and  $U$  cluster model parameters ( $\Delta < U$ ).<sup>30</sup> The average occupation of the V  $3d$  state, around 1.2, reflects the strong V  $3d$ -O  $2p$  covalent bonding (this occupation is much larger than the nominal  $d^0$  expected from a purely ionic model). The relatively large covalent contribution to the bonding in  $V_2O_5$  is in accordance with previous works.<sup>23</sup>

Figure 2 compares the cluster model (bottom) and band structure (top) calculations of  $V_2O_5$ . The zero in the energy scale corresponds to a Fermi level pinned at the bottom of the conduction band. The results of the band structure calculation are in very good agreement with previous studies.<sup>19,20</sup> The calculated band gap, about 2.2 eV, is in close agreement with the experimental value of 2.2–2.3 eV.<sup>7,8</sup> The occupation of the V  $3d$  orbitals obtained from the band structure calculation is about 1.6 (this value is slightly larger than that obtained from the cluster model calculation, around 1.2). The relatively large occupation of the V  $3d$  states indicates again the strong V  $3d$ -O  $2p$  hybridization.

TABLE IV. Contribution of the main configurations to the ground state of  $V_2O_5$ .

| Configuration | $V_2O_5$ ground state |  |
|---------------|-----------------------|--|
|               | Contribution          |  |
| $3d^0$        | 20%                   |  |
| $3d^1L$       | 47%                   |  |
| $3d^2L^2$     | 28%                   |  |

#### $V_2O_5$ Electronic Structure

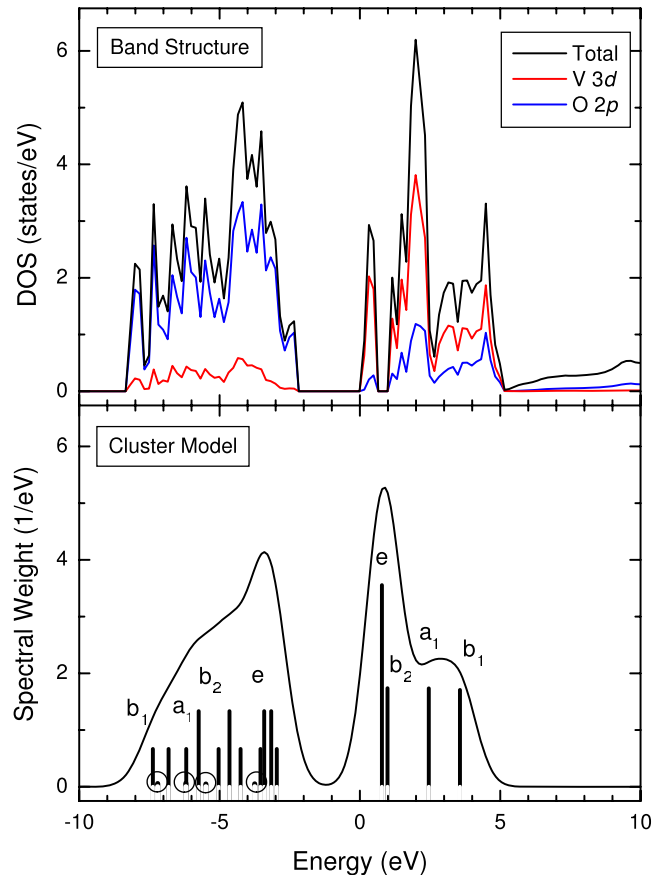


FIG. 2. (Color online) The spectral weight of  $V_2O_5$  from the cluster model compared to the density of states from the band structure calculation.

The occupied states in the valence band go from -8.3 to -2.2 eV, with a total width of about 6.1 eV. The main contribution to the valence band comes from the O  $2p$  states; the much smaller V  $3d$  state contribution is due to V-O hybridization. The unoccupied electronic states in the conduction band start at 0.0 eV and extend to higher energies. The conduction band is mostly formed by the V  $3d$  states from 0.0 to 5.1 eV, although there is some O  $2p$  character mixed in due to the V-O hybridization. The V  $3d$  band presents a split-off peak just above the Fermi level, which has an almost pure V  $3d$  character, as well as two stronger structures about 1.0–2.5 and 2.5–5.1 eV, which have a larger V  $3d$ -O  $2p$  admixture.

The cluster model calculation is a combination of the V  $3d$  removal and addition spectral weight. The O  $2p$  contribution was calculated in the square pyramid symmetry using a single particle approximation. The transitions were broadened with a 0.5 eV Gaussian to simulate band dispersion and energy resolution. The transitions from -7.4 to 3.0 eV are mostly related to the removal of an O  $2p$  electron (where the main contribution to the final state  $\Phi_f$  is given by the  $3d^0L$  configuration). These transitions are split due to the V  $3d$ -O  $2p$  and O  $2p$ -O  $2p$  interactions within the  $VO_5$  pyramid. On the other hand, the transitions from 1.3 to 4.1 eV correspond mainly to the addition of a V  $3d$

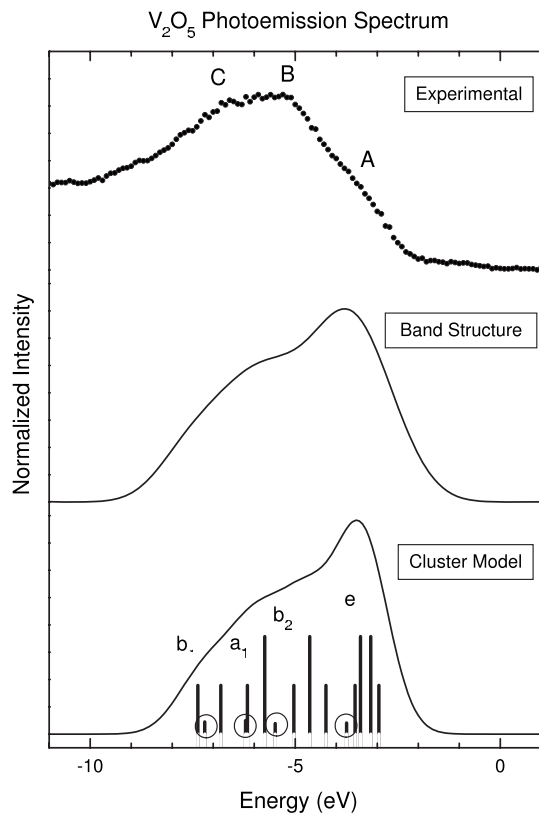


FIG. 3. Photoemission spectrum of  $V_2O_5$  taken at 50 eV compared to the total DOS (band structure) and the spectral weight (cluster model).

electron (where the main contribution to the final state  $\Phi_f$  is given by the  $3d^1$  configuration). These transitions are affected by the  $V 3d-O 2p$  interactions and crystal field effects (the peaks at 0.8, 1.0, 2.4, and 3.6 eV are related to the addition of an  $e$ ,  $b_2$ ,  $a_1$ , and  $b_1$  electrons, respectively).

The first removal state, around 3.0 eV, corresponds to the removal of an  $O 2p$  electron with  $A_1$  symmetry. The first addition state, about 0.8 eV, corresponds to the addition of a  $V 3d$  electron with  $E$  symmetry. The lowest energy optical excitation is thus of the  $p-d$  type, as expected in the charge-transfer regime.<sup>30</sup> This is in agreement with the assignment of the lower energy features in the reflectance spectrum.<sup>9</sup> The resulting band gap, about 2.5 eV, is slightly larger than the experimental value, 2.2–2.3 eV.<sup>7,8</sup> The calculated band gap increases with both the charge-transfer energy  $\Delta$  and the  $pd\sigma$  hybridization.

Figure 3 compares the experimental photoemission spectrum of  $V_2O_5$  to the calculated spectral weight, as well as the total density of states (DOS) broadened with a 0.5 eV Gaussian to simulate the energy resolution (the  $V 3d$  and  $O 2p$  states were equally weighted because their corresponding cross sections are similar).<sup>31</sup> The experimental spectrum is in agreement with previous results,<sup>9–11</sup> and the total DOS is similar to previous LDA<sup>19,20</sup> and density functional theory (DFT) results.<sup>22</sup> The main contribution to the valence band spectrum of  $V_2O_5$  is given by the removal of  $O 2p$  electrons. The experimental spectrum presents three main substructures: The first feature (A) is assigned to almost pure  $O 2p$

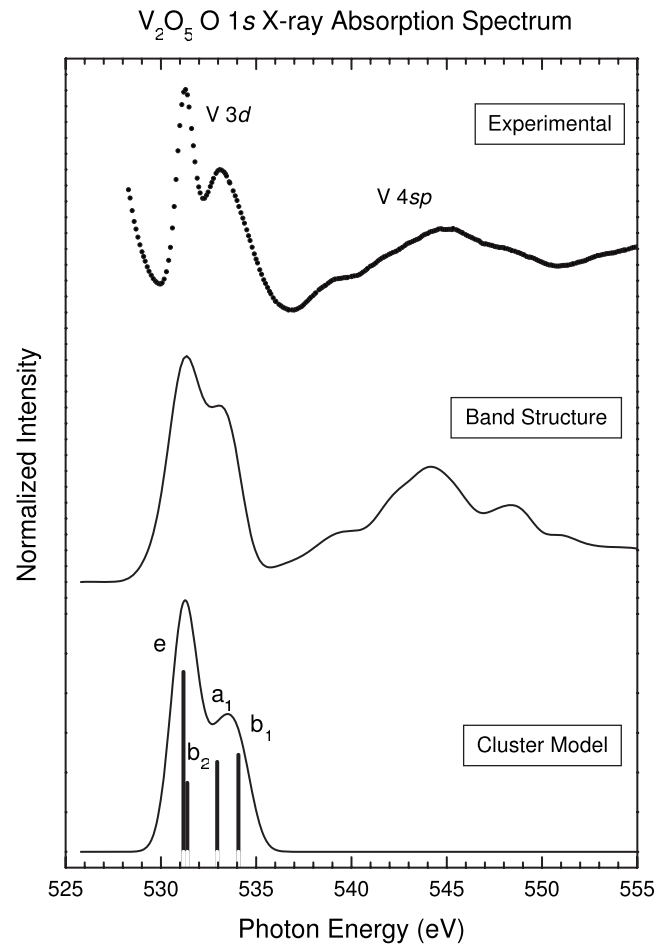


FIG. 4.  $O 1s$  x-ray absorption spectrum of  $V_2O_5$  compared to the  $O 2p$  DOS (band structure) and the  $O 2p$  spectral weight (cluster model).

nonbonding states, whereas the next two structures (B and C) are attributed to  $V 3d-O 2p$  bonding states.

The above assignments are in agreement with the cluster model and band structure calculations. The band structure presents a relatively nonbonding  $O 2p$  band around the A feature, from  $-2.2$  to  $-4.8$  eV, whereas the  $V 3d-O 2p$  bonding mixture is relatively larger in the B-C region, from  $-4.8$  to  $-8.3$  eV. The cluster model spectrum also presents pure  $O 2p$  removal states around the A feature, from  $-3.0$  to  $-5.0$  eV, as well as mixed  $V 3d-O 2p$  removal states in the B-C region, from  $-5.8$  to  $-7.4$  eV. Finally, the small peaks around  $-3.7$ ,  $-5.5$ ,  $-6.2$ , and  $-7.2$  eV correspond to the  $V 3d$  removal spectrum.

The cluster model and band structure results reproduce the positions of the structures in the spectra. The B and C structures in the photoemission spectrum are relatively enhanced with respect to the calculation. This spectrum was taken with a photon energy, which corresponds to the  $V 3d-V 3d$  resonance. The larger intensity of these features is thus attributed to the resonance of the  $V 3d-O 2p$  bonding states.<sup>9</sup> On the other hand, the present calculation is in good agreement with the off-resonance spectrum taken at 100 eV.<sup>11</sup>

Figure 4 compares the experimental  $O 1s$  x-ray absorption

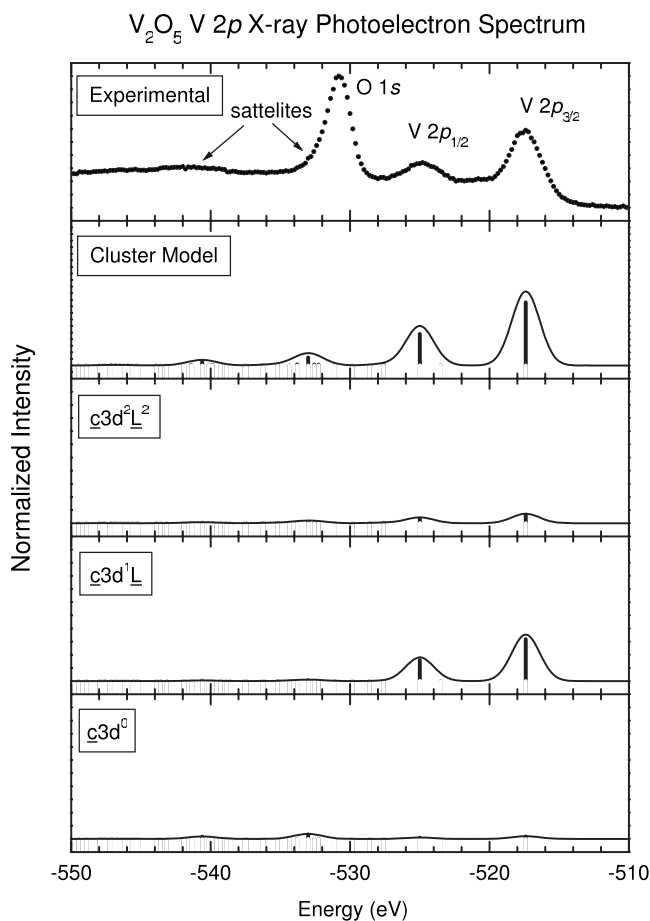


FIG. 5. V  $2p$  x-ray photoelectron spectrum of  $V_2O_5$  compared to the cluster model spectral weight projected into the main final state configurations.

spectrum of  $V_2O_5$  to the calculated spectral weight, as well as the O  $2p$  DOS broadened with a 0.6 eV Gaussian to simulate the energy resolution. The experimental spectrum is in agreement with previous results,<sup>12,13</sup> and the O  $2p$  DOS is similar to previous LDA<sup>19,20</sup> and DFT results.<sup>21</sup> The band structure and cluster model calculations reproduce very well the main features in the experiment. The O  $1s$  x-ray absorption spectrum corresponds to transitions from the O  $1s$  level to unoccupied O  $2p$  states. The first region, from 529 to 536 eV, is related to the O  $2p$  character mixed with V  $3d$  states, whereas the second region, from 536 to 551 eV, corresponds to the O  $2p$  character mixed with V  $4sp$  states. The V  $3d$  region is split by the pyramidal crystal field effects into two subbands around 531 and 533 eV. The first subband corresponds to final states of  $e$  and  $b_2$  symmetries, whereas the second subband is related to final states of  $a_1$  and  $b_1$  symmetries. The intensity of the  $a_1$  and  $b_1$  peaks is larger than in the addition state because of the larger V  $3d$ -O  $2p$  mixing.

Figure 5 compares the V  $2p$  x-ray photoelectron spectra of  $V_2O_5$  to the cluster model calculation. The calculated spectrum was projected into the main final state configuration, and the discrete transitions were broadened with a 0.9 eV Gaussian. The V  $2p$  level is split by the spin-orbit interactions into the V  $2p_{3/2}$  ( $\sim 517$  eV) and V  $2p_{1/2}$

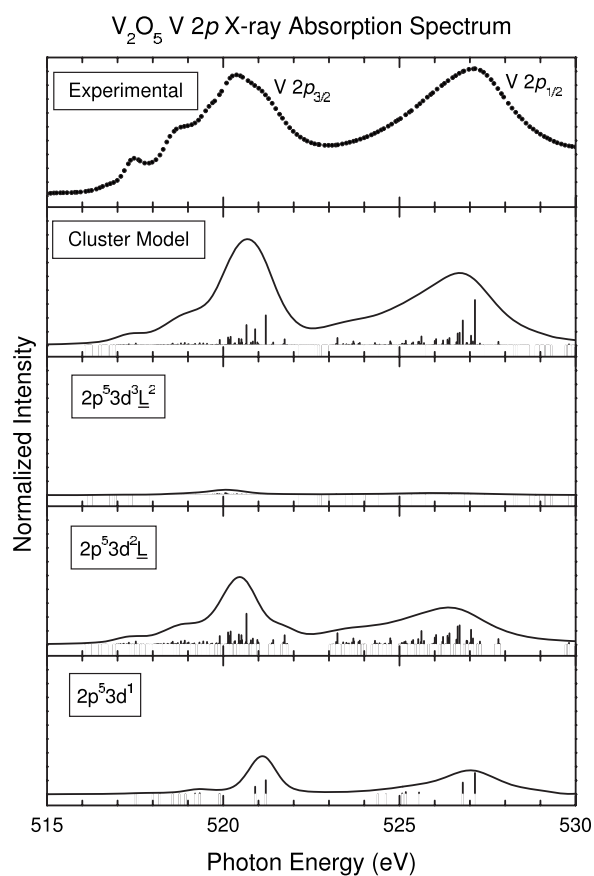


FIG. 6. V  $2p$  x-ray absorption spectrum of  $V_2O_5$  compared to the cluster model spectral weight projected into the main final state configurations.

( $\sim 525$  eV) peaks. The V  $2p_{3/2}$  and V  $2p_{1/2}$  main peaks presents charge-transfer satellites around 533 and 540 eV, respectively (the charge-transfer satellite corresponding to the V  $2p_{3/2}$  peak is hidden beneath the much stronger O  $1s$  peak).

The calculation is in good agreement with the experiment and reproduces the energy and intensity of the different features in the spectrum. The main peaks are mostly due to the so called *well screened*  $c3d^1L$  configuration (where  $c$  denotes a hole in the core level), whereas the satellites are mainly related to the *poorly screened*  $c3d^0$  configuration. The large O  $2p$  contribution to the main peaks indicates again the strong V  $3d$ -O  $2p$  covalent interactions. Finally, the charge-transfer satellite represents a many-body effect in a nominal  $3d^0$  compound.

Figure 6 compares the V  $2p$  x-ray absorption spectrum of  $V_2O_5$  to the cluster model calculation. The calculated spectrum was also projected into the main final state configurations, and the transitions were broadened with a 0.4 eV (0.3 eV) Gaussian (Lorentzian). The V  $2p$  level is again split by spin-orbit interactions into the V  $2p_{3/2}$  (from 516 to 522 eV) and the V  $2p_{1/2}$  (from 522 to 530 eV) absorption edges. The spectrum is related to V  $2p \rightarrow V 3d$  transitions and is dominated by multiplet and crystal field effects.<sup>32,33</sup> The Slater integrals were reduced to 80% of their atomic values, and the  $C_{4v}$  crystal field parameters (Dq, Dt,



and Ds) are listed in Table II (the experimental spectrum cannot be reproduced by a calculation in a crystal field of  $O_h$  symmetry).

The calculation is in good agreement with the experiment and reproduces the main features in the spectrum. The spectral weight is dominated by the  $2p^5 3d^2 \underline{L}$  final state configuration, with a relative weight of 69%, whereas the relative contribution from the  $2p^5 3d^1$  final state configuration is about 25%. This is related to the much larger contribution of the  $3d^1 \underline{L}$  configuration to the ground state because the  $2p^5 3d^2 \underline{L}$  final state configuration is reached via  $2p^6 3d^1 \underline{L} \rightarrow 2p^5 3d^2 \underline{L}$  transitions. This result illustrates again the importance of the large V  $3d-O 2p$  covalent interactions, as well as the influence of many-body effects even in a nominal  $3d^0$  compound.

The above results provide a complete description of the electronic structure of the  $V_2O_5$  compound. The cluster model calculation explains both the core- and valence-level spectra with a single parameter set. The present results confirm that the V  $3d-O 2p$  covalent interaction plays a dominant role in the  $V_2O_5$  material. The calculated V  $2p$  x-ray photoelectron spectrum shows clear satellites due to many-body effects (this shows that electron correlation effects are also important in a nominal  $3d^0$  compound such as  $V_2O_5$ ). The calculated V  $2p$  x-ray absorption spectrum is sensitive to

the reduced symmetry of the crystal field. These two effects are thus crucial for a proper description of the electronic structure of the  $V_2O_5$  oxide.

## V. SUMMARY AND CONCLUSIONS

In summary, we studied the electronic structure of the  $V_2O_5$  compound using cluster model calculations. The calculations included the strong V  $3d-O 2p$  interactions, the many-body effects, and the reduced symmetry of the  $V^{5+}$  ions. The ground state is highly covalent and is dominated by the  $3d^1 \underline{L}$  configuration with a relative weight of about 47%. This compound is in the charge-transfer regime, and the lowest energy optical excitations are of the  $p-d$  type. The value of the calculated band gap, 2.2–2.5 eV, is in good agreement with the experimental result, 2.2–2.3 eV. The cluster model results are in good agreement with band structure calculations. They also reproduce reasonably well both the core- and valence-level spectra of the  $V_2O_5$  material. The present results confirm the importance of the strong V  $3d-O 2p$  covalent interactions. The results also indicate the influence of many-body effects and the reduced symmetry of the  $V^{5+}$  ions. These effects are crucial for a proper description of the electronic structure of the  $V_2O_5$  compound.

\*miguel@fisica.ufpr.br

<sup>1</sup>F. Morin, Phys. Rev. Lett. **3**, 34 (1959).

<sup>2</sup>J. B. Bates, N. J. Dudley, D. C. Lubben, G. R. Gruzalski, B. S. Kwak, Xiaohua Yu, and R. A. Zuhr, J. Power Sources **54**, 58 (1995).

<sup>3</sup>A. Talledo and C. G. Granqvist, J. Appl. Phys. **77**, 4655 (1995).

<sup>4</sup>J. Livage, Chem. Mater. **3**, 578 (1991).

<sup>5</sup>G. C. Bond and S. F. Tahir, Appl. Catal. **71**, 1 (1991).

<sup>6</sup>R. Enjalbert and J. Galy, Acta Crystallogr., Sect. C: Cryst. Struct. Commun. **42**, 1467 (1986).

<sup>7</sup>S. F. Cogan, N. M. Nguyen, S. J. Perrotti, and R. D. Rauh, J. Appl. Phys. **66**, 1333 (1989).

<sup>8</sup>E. E. Chain, Appl. Opt. **30**, 2782 (1991).

<sup>9</sup>S. Shin, S. Suga, M. Taniguchi, M. Fujisawa, H. Kanzaki, A. Fujimori, H. Daimon, Y. Ueda, K. Kosuge, and S. Kachi, Phys. Rev. B **41**, 4993 (1990).

<sup>10</sup>R. Zimmermann, R. Claessen, F. Reinert, P. Steiner, and S. Hüfner, J. Phys.: Condens. Matter **10**, 5697 (1998).

<sup>11</sup>S. Laubach, P. C. Schmidt, A. Thissen, F. J. Fernandez-Madrigal, Q.-H. Wu, W. Jaegermann, M. Klemm, and S. Horn, Phys. Chem. Chem. Phys. **9**, 2564 (2007).

<sup>12</sup>M. Abbate, H. Pen, M. T. Czyzyk, F. M. F. de Groot, J. C. Fuggle, Y. J. Ma, C. T. Chen, F. Sette, A. Fujimori, Y. Ueda, and K. Kosuge, J. Electron Spectrosc. Relat. Phenom. **62**, 185 (1993).

<sup>13</sup>E. Goering, O. Muller, M. Klemm, M. L. den Boer, and S. Horn, Philos. Mag. B **75**, 229 (1997).

<sup>14</sup>Z. M. Zhang and V. E. Henrich, Surf. Sci. **321**, 133 (1994).

<sup>15</sup>S. P. Freidman, V. M. Cherkashenko, V. A. Gubanov, E. Z. Kurmaev, and V. L. Volkov, Z. Phys. B: Condens. Matter **46**, 31 (1982).

<sup>16</sup>O. Sipr, A. Simunek, S. Bocharov, T. Kirchner, and G. Drager, Phys. Rev. B **60**, 14115 (1999).

<sup>17</sup>S. Stizza, G. Mancini, M. Benfatto, C. R. Natoli, J. Garcia, and A. Bianconi, Phys. Rev. B **40**, 12229 (1989).

<sup>18</sup>S. Atzkern, S. V. Borisenko, M. Knupfer, M. S. Golden, J. Fink, A. N. Yaresko, V. N. Antonov, M. Klemm, and S. Horn, Phys. Rev. B **61**, 12792 (2000).

<sup>19</sup>V. Eyert and K.-H. Höck, Phys. Rev. B **57**, 12727 (1998).

<sup>20</sup>A. Chakrabarti, K. Hermann, R. Druzinic, M. Witko, F. Wagner, and M. Petersen, Phys. Rev. B **59**, 10583 (1999).

<sup>21</sup>C. Kolczewski and K. Hermann, Surf. Sci. **552**, 98 (2004).

<sup>22</sup>K. Hermann, M. Witko, R. Druzinic, A. Chakrabarti, B. Tepper, M. Elsner, A. Gorschlüter, H. Kühlenbeck, and H. J. Freund, J. Electron Spectrosc. Relat. Phenom. **98-99**, 245 (1999).

<sup>23</sup>A. E. Bocquet, T. Mizokawa, K. Morikawa, A. Fujimori, S. R. Barman, K. Maiti, D. D. Sarma, Y. Tokura, and M. Onoda, Phys. Rev. B **53**, 1161 (1996).

<sup>24</sup>G. van der Laan, C. Westra, C. Haas, and G. A. Sawatzky, Phys. Rev. B **23**, 4369 (1981).

<sup>25</sup>A. Fujimori and F. Minami, Phys. Rev. B **30**, 957 (1984).

<sup>26</sup>R. J. O. Mossaneck and M. Abbate, Phys. Rev. B **74**, 125112 (2006).

<sup>27</sup>R. J. O. Mossaneck and M. Abbate, Phys. Rev. B **75**, 115110 (2007).

<sup>28</sup>S. Y. Savrasov, Phys. Rev. B **54**, 16470 (1996).

<sup>29</sup>S. H. Vosko, L. Wilk, and M. Nusair, Can. J. Phys. **58**, 1200 (1980).

<sup>30</sup>J. Zaanen, G. A. Sawatzky, and J. W. Allen, Phys. Rev. Lett. **55**, 418 (1985).

<sup>31</sup>J. J. Yeh and I. Lindau, At. Data Nucl. Data Tables **32**, 1 (1985).

<sup>32</sup>M. Abbate, G. Zampieri, J. Okamoto, A. Fujimori, S. Kawasaki, and M. Takano, Phys. Rev. B **65**, 165120 (2002).

<sup>33</sup>M. Abbate, L. Moggi, F. Prado, and A. Caneiro, Phys. Rev. B **71**, 195113 (2005).